



Based on Haar-like feature and improved YOLOv4 navigation line detection algorithm in complex environment

Shenqi Gao, Shuxin Wang, Weigang Pan, Mushu Wang, Song Gao

Shenqi Gao

School of Information Science and Electrical Engineering
Shandong Jiaotong University, China
Shandong, Jinan, 250357, Chian
feize0624@163.com

Shuxin Wang

School of Information Science and Electrical Engineering
Shandong Jiaotong University, China
Shandong, Jinan, 250357, Chian
bestariver@163.com

Weigang Pan*

School of Rail Transportation
Shandong Jiaotong University, China
*Corresponding author: panweigang1980@163.com

Mushu Wang

School of Information Science and Electrical Engineering
Shandong Jiaotong University, China
Shandong, Jinan, 250357, Chian
wangmushu@126.com

Song Gao

School of Information Science and Electrical Engineering
Shandong Jiaotong University, China
Shandong, Jinan, 250357, Chian
gaosong@sdjtu.edu.cn

Abstract

In order to improve the detection accuracy of the navigation line by the unmanned automatic marking vehicle (UAMV) in the complex construction environment. Solve the problem of unqualified road markings drawn by the UAMV due to inaccurate detection during construction. A navigation line detection algorithm based on and improved YOLOv4 and improved Haar-like feature named YOLOv4-HR is proposed in this paper. Firstly, an image enhancement algorithm based on improved Haar-like features is proposed. It is used to enhance the images of the training set, make the images contain more semantic information, which improves the generalization ability

of the network; Secondly, a multi-scale feature extraction network is added to the YOLOv4 network, which made model has a stronger learning ability for details and improves the accuracy of detection. Finally, a verification experiment is carried out on the self-built data set. The experimental results show that, compared with the original YOLOv4 network, the method proposed in this paper improves the AP value by 14.3% and the recall by 11.89%. The influence of factors such as the environment on the detection effect of the navigation line is reduced, and the effect of the navigation line detection in the visual navigation of the UAMV is effectively improved.

Keywords: Haar-like feature, YOLOv4, image enhancement, driverless, visual navigation.

1 Introduction

Highway road marking construction has heavy construction task, and the workers will inhale a large amount of volatile gas from paint during long time construction, that seriously endanger the health of workers. Therefore, it is very necessary to research the navigation algorithm of the UAMV under the modern conditions, and promote the development of the UAMV. Due to on the road under construction, there are no visual navigation targets such as lane line and traffic sign. At present, in the construction of highway road marking, the navigation line (The navigation line is a straight line drawn on the road used white paint to guide the road marking construction) is the only suitable visual navigation target for the UAMV. The UAMV locates and navigates by identifying the navigation line and then carries out road marking construction. And the object detection also is one of the core tasks in visual navigation [21][10].Therefore, whether the navigation line can be accurately identified is one of the important factors affecting the construction accuracy of the UAMV. However, the detection of navigation line is a challenging task. Factors such as the shape of the navigation line, dust pollution, light intensity, and shadows will affect the detection results of the navigation line. More importantly, in-vehicle computing platforms often have limited performance. Due to this, complex algorithms cannot be deployed, which is also one of the factors that limit detection accuracy. Based on the above problems, this paper proposed a navigation line detection algorithm suitable for UAMV. The innovation of this paper lies in two aspects.

(1) In order to improve the generalization ability of the model, this paper proposed an image enhancement method based on improved Haar-like features.

(2) Based on the YOLOv4 network, this paper adds a multi-scale feature extraction network, fusing high-level features with low-level features to capture more detailed information and improves the detection effect of the model.

By applying the image enhancement method and improved the network of YOLOv4 these studies to UAMV, it can effectively improve the effect of model detection and the accuracy of navigation. Promote the development of unmanned automatic marking construction technology.



Figure 1: Unmanned automatic marking vehicle

2 Related work

In unmanned driving technology, the navigation methods include lidar [17], millimeter wave radar[28], vision, etc. The millimeter-wave radar is often used for map construction. Lidar can detect the markings on the road through the reflection intensity of pulsed laser [23]. However, the width of the navigation line is narrow and the ability to reflect pulsed laser is weak, so it cannot be detected by lidar. Compared with other sensors, vision sensors have fast response, high precision and low price, and can accurately collect effective information such as brightness, color, and texture of the navigation line. However, the detection effect of vision-based navigation algorithms is affected by factors such as illumination, road surface, and weather conditions, which brings great challenges to navigation tasks in outdoor scenes. Therefore, it is of great engineering significance to design an accurate and reliable navigation line detection algorithm.

Vision-based unmanned navigation mostly uses lane lines as the navigation target [12], and the navigation line can be approximated as narrow and inconspicuous lane line. About the detection algorithms, the traditional lane line detection algorithms [24][25][13][16] often only have a good detection effect in a single definite scene, and lack adaptability to different scenes. In the case of complex environment and serious interference, the robustness and detection accuracy of traditional detection algorithms are obviously insufficient., With the improvement of hardware computing power and the improvement of neural network theory, deep learning has made breakthroughs in the field of target detection [7]. Target detection algorithms based on convolutional neural networks [29][20][6][30][31] have achieved better recognition results than traditional algorithms in various datasets. The YOLO model has been widely used in driverless navigation due to its advantages of fast detection speed and high detection accuracy [14]. In the unmanned navigation algorithms, Xing-Yu Ye [26] et al. proposed a two-stage YOLOv2 method to detect lane markings, which improved the detection accuracy, but the detection speed of the two-stage algorithm would be reduced. Seong-Eun Ryu [19] et al. used hard-example mining and augmentation policy optimization combined with YOLO to improve the detection ability for occluded lane markings, but the parameters of the optimization strategy used were still manually determined. Wei Yang [27] et al. aimed at the problem that it is difficult to detect when the edge area of the lane line is occluded or deformed, combined YOLOv3 with long short-term memory and recurrent neural network, improves the detection accuracy. But too much network fusion increases the detection time and cannot meet the real-time requirements. Haris, M [8] et al. proposed a lane line prediction model BGRU-Lane based on lane line distribution, and the dempster-Shafer algorithm was used to integrate the results of BGRU-L and Improved YOLOv3 to improve the lane line detection ability under complex environments. YuCheng Fan [4] et al. combined lidar detection in unmanned driving technology with YOLOv4, and proposed the LS-R-YOLOv4 algorithm, which improved the accuracy of target detection in unmanned driving. R Kavya [11] et al. used YOLOv4 for real-time object detection in advanced driver assistance systems. Yingfeng Cai [2] et al. proposed the YOLOv4-5D algorithm for real-time target detection of driverless vehicles. The authors improved the network structure of YOLOv4, and used an optimized network pruning algorithm for network pruning, which improved the network detection effect and detection speed. Ding Y et al. [3] proposed a lane line detection method based on YOLOv4. Lane line detection in complex environments realized, but there are certain limitations in detecting inclined lane lines. Zhang [32] et al. proposed a crosswalk detection network based on YOLOv5, which improved the detection accuracy in complex environments.

Due to the narrow width of the navigation line and the indistinguishable of the navigation line and the background in the construction environment, the CNN cannot accurately extract the local texture features and edge information. Using image enhancement methods such as random cropping, flipping, dropout, and batch normalization [9][18] in the detection model can effectively improve the detection effect of CNN. that can be extracted from the Haar-like template are suitable for targeted feature extraction in single target detection, while the high-level features extracted by CNN are robust and scale invariant. Fusion of Haar-like features in CNN can effectively enhance the performance of the model.

The Haar-like features are first used for face detection [22]. And in recent studies, the use of Haar-like features combined with deep convolutional neural networks has been widely used in the

improvement of network models. Jiaqiu Ai [1] et al. proposed a ship detection algorithm based on multi-scale rotation-invariant Haar-like feature integrated convolutional neural network. The Haar-like features are used to improve the problem of losing local texture and edge information that are important for target recognition when conventional CNN extracts deep features. Keyu Lu [15] et al. proposed a convolutional neural network based on a generalized Haar-like filter, which used a generalized Haar-like filter to balance the parameters and size of the neural network. However, the Haar-like template of the network is obtained in a data-driven way, which may not achieve ideal results when performing other target detections. Jihong Guo [5] et al. used extended Haar-like features, AdaBoost combined with convolutional neural network to detect wind turbine blade damage to improve the detection accuracy.

The Haar-like feature is very sensitive to the grayscale changes of the image, so the Haar-like feature is very suitable for the enhancement of the navigation line image. According to the feature of the navigation line, this paper improved the original Haar-like feature, and proposed an image enhancement method based on the improved Haar-like feature. And a multi-scale feature extraction network is increased to the YOLOv4 model. Through the above methods effectively improves the generalization ability of the model and the accuracy of detection.

3 Based on Haar-like feature and improved YOLOv4 road marking construction navigation line detection algorithm

3.1 Based on improved Haar-like feature image enhancement algorithm

In this section, a Haar-like feature template with a buffer is proposed to improve the of feature extraction effect of uneven width and rough edge navigation line

3.1.1 Improved Haar-like feature template

Haar-like is a local texture feature descriptor which reflects the change of image grayscale and can capture the structure information. Compared with other feature operators, Haar-like features are scalable and fast to calculate, reducing intra-class variance while increasing inter-class variance [32], which makes it particularly sensitive to edge and texture features of the image.

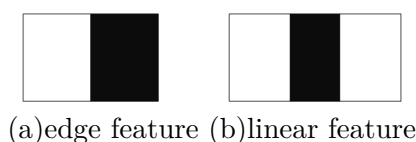


Figure 2: Basic Haar-like feature template

In this paper, a buffer is added to the basic Haar-like feature template, as shown in figure 3. The improved template is consisted of black area, white area and gray area. Where the grey area is the buffer region, it allows the template to skip the part where the edge of the navigation line is mixed with the background. So that the discontinuity and burr of the navigation line edge can be ignored in feature extraction. Therefore, in the process of feature extraction, the improved template can more highlight the main features of the navigation line, and the interference due to the noise of the navigation line edge to the feature extraction is reduced. Thus, the effect of feature extraction is improved.

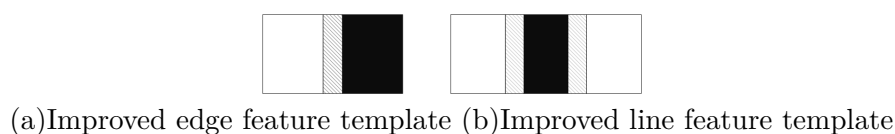


Figure 3: The Haar-like feature template proposed in this paper

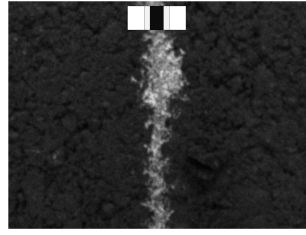


Figure 4: The schematic diagram of feature extraction

3.1.2 Haar-like feature calculation

In order to extract Haar-like features, first, the navigation line image is converted to a grayscale image and integral image operation is used to improve the efficiency of the algorithm. The calculation process of the algorithm is as follows: the upper left corner of the image is defined as the origin (0,0), and the value of the integral image is obtained by equation (1).

$$I(i, j) = \sum_{k < i, l < j} img(k, l) \tag{1}$$

Where, (i, j) are the number of rows and columns of the image pixel, *img* is the grayscale image of the original image. When the integral image is constructed, the sum of pixels in any rectangular region of the image can be obtained by simple operations. In figure 5, the pixel of area A can be calculated by equation (2).

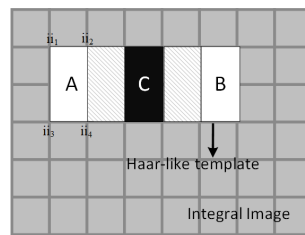


Figure 5: The schematic diagram of Improved Haar-like feature calculation

$$\sum_{(i,j) \in R_w} I(i, j) = ii_1 + ii_2 - (ii_3 + ii_4) \tag{2}$$

After the pixel sum of different regions is calculated, The Haar-like feature can be calculated by equation (3). In the template proposed in this paper, only the values of the black and white areas are calculated, and the values of the buffer are not calculated.

$$f = \sum_{(i,j) \in R_w} I(i, j) - 2 \times \sum_{(i,j) \in R_B} I(i, j) \tag{3}$$

Where, R_B represents the region of black, R_w represents the region of white, $\sum_{(i,j) \in R_w} I(i, j)$ is the value of the white region of the integral image, $\sum_{(i,j) \in R_B} I(i, j)$ is the value of the black region of the integral image, the f is the Haar-like feature value.

3.1.3 Normalization processing

Because the obtained feature value has negative values and too large values, in order to compress the range of value, the obtained feature value need to be normalized. In this algorithm, gamma transform is used for normalization.

$$\begin{aligned}
 s &= cr^\gamma \\
 c &= 255/\max(\text{pix})^\gamma
 \end{aligned}
 \tag{4}$$

where, r is the input value of the grayscale image, c is the grayscale scaling factor, $\max(\text{pix})$ is the maximum value of the pixel in the grayscale image, and γ is the gamma factor.

Arrange the feature value according to the corresponding indexes to form a feature image, and the feature value are normalized to $[0,255]$ by using equation (5). The finally feature image as shown in figure 6.

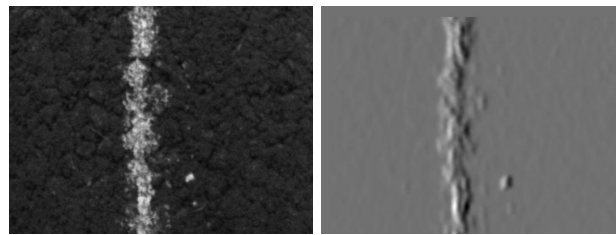


Figure 6: Original image and feature image

3.1.4 Fusion enhancement

Feature-level fusion is used for image enhancement in this algorithm. The method is, combine the gray image of original image with the feature image extracted by multi-scale template to form a three-channel feature fusion image. The main purpose of this is to reduce the influence of background and enhance the features of the navigation line. The channel splicing method is linear splicing. The schematic diagram of image fusion is shown in figure 7, and the overall flow chart of the algorithm is shown in figure 8.

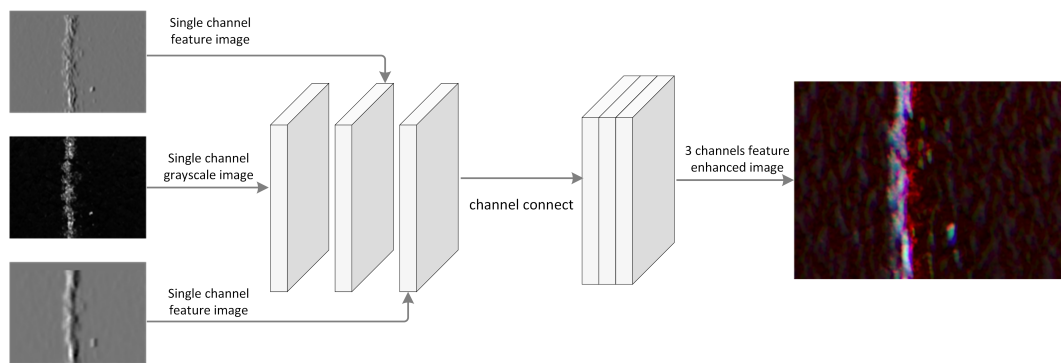


Figure 7: Schematic diagram of image fusion.

3.2 Improved YOLOv4 network

In the problem of detecting navigation line, in order to improve the generalization ability of the model and make the model can accurately detect the navigation line in complex environment, the structure of YOLOv4 network is improved in this paper.

On the basis of the original YOLOv4 network, a multi-scale feature extraction network is added in parallel. First, the multi-scale feature extraction network extracts low-level features, while YOLOv4 extracts high-level features. Then the two features are fused to make up for the problem of information loss caused by the deep network, thereby improving the detection effect of the model.

The main part of the feature extraction network consists of three layers of convolution and pooling. In this network, input is the gray image of navigation line. Firstly, three different scales of Haar-like templates are used to extract features and get the feature images. Then, the 3×3 convolution and

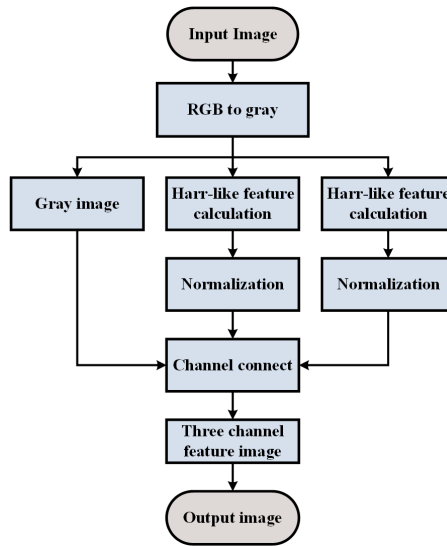


Figure 8: Algorithm flow chart

maximum pooling are used for feature images. The batch normalization (BN) is used for normalization after each layer of convolution, using Mish self-regularizing nonmonotonic neural as activation function. Finally, the output feature with same dimension of the YOLO head is obtained, which is recorded as \hat{U}_n . The YOLO head which is recorded as \hat{V}_n . Then the feature output is linearly spliced with the YOLO head, that is

$$F_n = \hat{U}_n + \hat{V}_n \tag{5}$$

Where, F_n is the output of the network after linear splicing.

After feature linear splicing, 3×3 convolution operation has been used to reduce the aliasing effect. The network structure is shown in figure 9.

The parameters of the multi-scale feature extraction networks are shown in table 1, where H and W are the dimensions of the input image, both are 416.

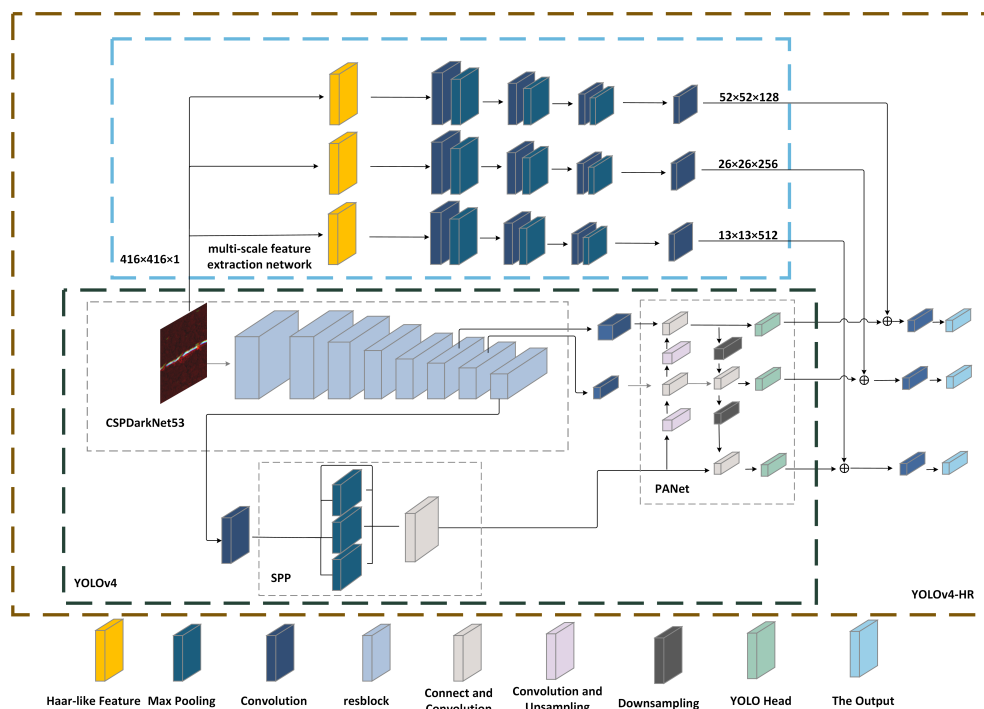


Figure 9: The network structure of YOLOv4-HR

Table 1: The parameters of YOLOv4-HR

Input	Operator	Channel	Output
$416 \times 416 \times 1$	Haar-like feature extraction	size	$416 \times 416 \times 1$
$416 \times 416 \times 1$			$416 \times 416 \times 1$
$416 \times 416 \times 1$			$416 \times 416 \times 1$
$416 \times 416 \times 1$	Convolution	16	$416 \times 416 \times 16$
$416 \times 416 \times 1$		32	$416 \times 416 \times 32$
$416 \times 416 \times 1$		64	$416 \times 416 \times 64$
ditto	Mish and BN	-	ditto
$416 \times 416 \times 16$	Max Pooling	-	$208 \times 208 \times 16$
$416 \times 416 \times 32$			$104 \times 104 \times 32$
$416 \times 416 \times 64$			$104 \times 104 \times 64$
$208 \times 208 \times 16$	Convolution	64	$208 \times 208 \times 32$
$104 \times 104 \times 32$		128	$104 \times 104 \times 64$
$104 \times 104 \times 64$		256	$104 \times 104 \times 128$
ditto	Mish and BN	-	ditto
$208 \times 208 \times 32$	Max Pooling	-	$104 \times 104 \times 32$
$104 \times 104 \times 64$			$52 \times 52 \times 64$
$104 \times 104 \times 128$			$26 \times 26 \times 128$
$104 \times 104 \times 32$	Convolution	64	$104 \times 104 \times 64$
$52 \times 52 \times 64$		128	$52 \times 52 \times 128$
$26 \times 26 \times 128$		256	$26 \times 26 \times 256$
ditto	Mish and BN	-	ditto
$104 \times 104 \times 64$	Max Pooling	-	$52 \times 52 \times 64$
$52 \times 52 \times 128$			$26 \times 26 \times 128$
$26 \times 26 \times 256$			$13 \times 13 \times 256$
$52 \times 52 \times 64$	Convolution	128	$52 \times 52 \times 128$
$26 \times 26 \times 128$		256	$26 \times 26 \times 256$
$13 \times 13 \times 256$		512	$13 \times 13 \times 512$
ditto	Mish and BN	-	ditto

4 Experiment

In this section, the detection experiment is carried out using the navigation line images not included in the training set. The accuracy of the method proposed in this paper is verified by comparative experiments, and the experimental results are analyzed.

4.1 The construction of training set and validation set

The training set used in this paper is a self-built data set, which is the asphalt pavement navigation line images taken on the various environments, which mainly include a total of 5487 images of different lengths, thicknesses, intermittent and normal navigation line under different backgrounds. The resolution of the images includes 640×480 and 1280×1024 . The types of images are shown in figure 10.

In order to verify the model trained by the algorithm proposed in this paper has good generalization ability. When constructing the validation set, the images that do not appear in the training set are selected. Including the blurred navigation line, vision-based inspection equipment edge light leakage, and the navigation line after rain, a total of 992 images. The types of images are shown in figure 11.

4.2 Experimental methods and results

All model training in the experiments is done on a server configured as Core Xeon E5-Gold 5218R@2.3GHz, 96GB RAM and 2080 super. During training, the resolution of the input image

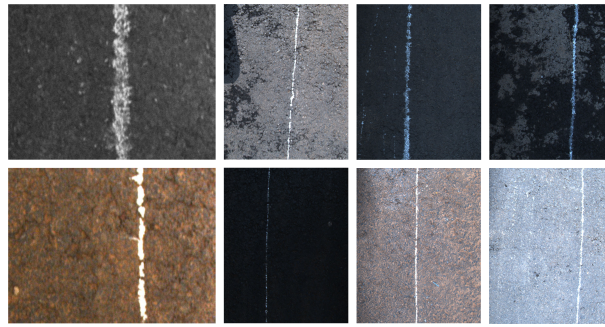


Figure 10: Images included in the training set

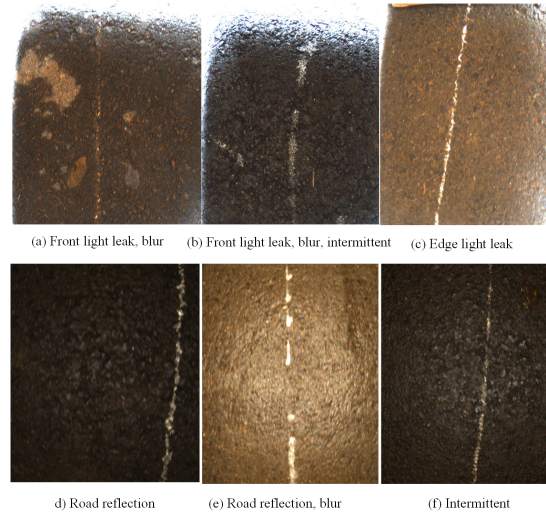


Figure 11: Images included in the validation set

is scaled to 416×416 , the batch size is set to 2, the epoch is set to 100, the ratio of 5487 images to the training set and the validation set is 9:1, and the learning rate is set to 0.001 when freezing training, the learning rate is set to 0.0001 when unfreezing training.

4.2.1 Comparison experiments of different Harr-like templates

In order to verify the effectiveness of the image enhancement algorithm proposed in this paper, several groups of comparative experiments were carried out. First different types of Haar-like templates are used for features extracted to image enhancement, then the enhanced images are used as the training set of the YOLOv4 network. The model obtained from training is verified on the validation set, the enhanced effect is shown in figure 12 and the experimental results are shown in table 2. The P-R curve comparison of the model is shown in figure 13.

Table 2: The effect of image enhancement by using different types of Haar-like features on model detection.

	AP	recall
YOLOv4	70.96%	68.68%
Edge feature	77.76%	68.87%
Line feature	81.01%	73.58%
Improved edge feature	81.53%	73.77%
Improved line feature	84.83%	76.79%

Analysis of the experimental data shows that, compared with the model trained without image enhancement algorithm, the AP of the model increases by 6.8% and the recall increases by 0.19%

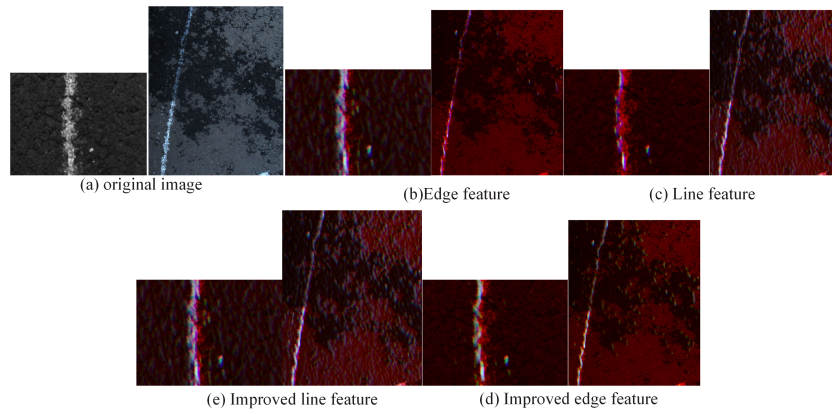


Figure 12: Enhanced effect

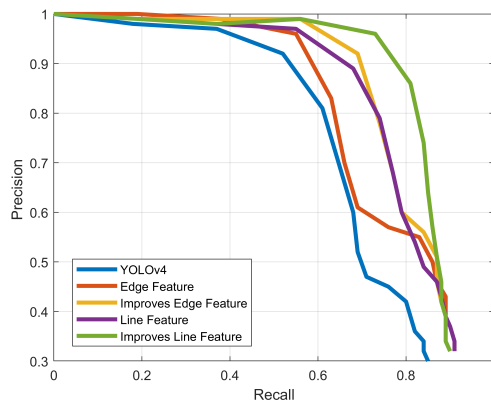


Figure 13: The comparison of P-R curve.

after image enhancement using edge features. And after using the edge feature with the buffer for image enhancement, the AP value of the model is increased by 10.57%, and the recall is increased by 4.9%. Using the linear feature with buffer for image enhancement, AP increased by 13.87% and recall increased by 8.11%. It can be seen that the improved template can effectively improve the effect of model detection, and the improved template proposed in this paper has a better enhancement effect, which verifies the effectiveness of the method.

In order to determine the impact of the combination of Haar-like features with different sizes in the image enhancement algorithm to the model detection effect. Linear feature with buffer Haar-like templates with sizes of 3, 7, 9, 12, 15, and 25 pixels were selected for combination. The enhanced effect is shown in figure 14, the experimental results are shown in table 3 and the P-R curve of the model obtained by training with different size template combinations is shown in the figure 15.

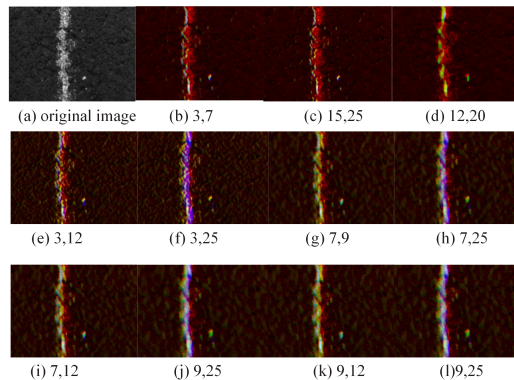


Figure 14: Enhanced effect

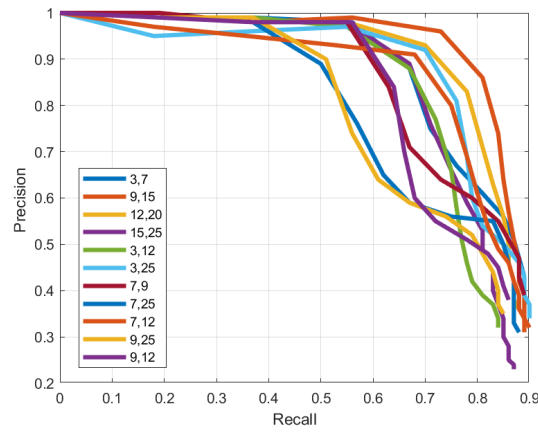


Figure 15: The comparison of P-R curve

Table 3: The effect of image enhancement algorithm using different sizes template combinations to the model detection effect

The combination of template size	AP	recall
3,7	80.74%	73.68%
3,12	76.36%	69.34%
3,25	80.97%	76.04%
7,9	78.42%	78.68%
7,12	79.15%	75.94%
7,25	71.31%	70.75%
9,15	84.83%	76.79%
9,25	70.88%	66.7%
9,12	74.91%	65.94%
15,25	77.68%	68.77%
12,20	82.3%	71.79%

4.2.2 Comparison experiments of different model

In this experiment, in order to verify the detection effect of YOLOv4-HR, it is compared with YOLOv3, Mobilenet-YOLOv4, YOLOv4. The experimental results are shown in table 4 and figure 16.

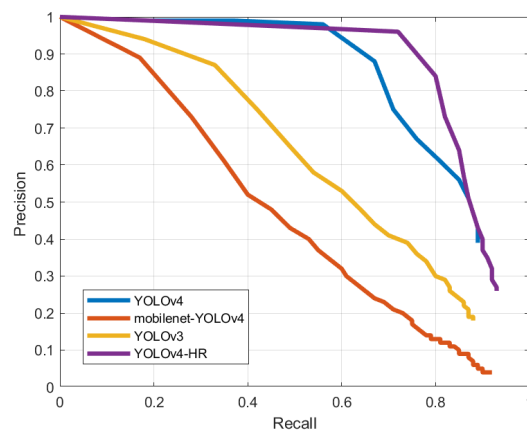


Figure 16: The comparison of P-R curve

Table 4: Comparison of the method proposed in this paper with other methods

Model	AP	Recall
YOLOV3	60.18%	25.57%
Mobilenet-YOLOv4	45.87%	31.04%
YOLOv4	70.96%	68.68%
YOLOv4-HR	85.09%	80.57%

For the original YOLOv4 network, due to YOLOv4-HR has added a multi-scale feature extraction network to extract shallow semantic information, which enables the network to extract richer multi-scale features, thereby improving the detection effect. Compared with the original YOLOv4 network, the AP value is increased by 14.3%, and the Recall is increased by 11.89%. The experimental results verify the feasibility of the method proposed in this paper.

The comparison of detection results on the validation set is shown in figure 17. In the case of blurred navigation line, side light leakage, front-end light leakage, etc. with serious interference, the YOLOv4 has the problem that it is easy to misidentify the light leakage side as the navigation line, and the detection rate of the blurred navigation line is low. While using the method proposed in this paper, the situation of misidentification is reduced, and the success rate of identifying fuzzy navigation line is improved. It is verified that the method proposed in this paper can effectively improve the generalization ability of the model, and can reduce the impact of the environment on the detection.

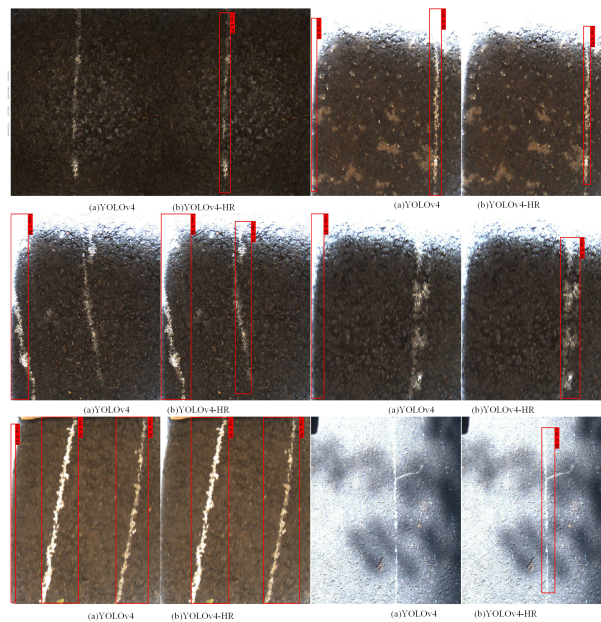


Figure 17: The comparison of detection results.

Conclusion

This paper proposed a navigation line detection method combining Haar-like feature and improved YOLOv4. First, an image enhancement method based on Haar-like features is proposed to highlight the subject features of the leading lines and reduce the influence of noise; in addition, a multi-scale feature extraction network is added to the YOLOv4 network to extract low-level features and enrich feature information. Experimental results on the self-built data sets show that the proposed approach has more accurate detection effect and stronger generalization ability compared with several methods.

In the current research, the size of the template of the image enhancement algorithm is still determined by experiments on existing data sets. However, in different environments, the model may not achieve the best detection effect on navigation line with different widths. Therefore, in the

practical applications and future theoretical research, it is necessary to study how to adaptively select the template size to make the model achieve the best detection effect.

Acknowledgment

This work was supported by the Major Science and Technology Innovation Project of Shandong Province (No.2020CXGC010110), Shandong Provincial Natural Science Foundation (No.ZR2022MF345) and Support Plan for Shandong Key Laboratory of Transportation Industry.

References

- [1] Ai, J.; Tian, R.; Luo, Q.; Jin, J.; Tang, B. (2019). Multi-scale rotation-invariant Haar-like feature integrated CNN-based ship detection algorithm of multiple-target environment in SAR imagery, *IEEE Transactions on Geoscience and Remote Sensing*, 57(12), 10070–10087, 2019.
- [2] Cai, Y.; Luan, T.; Gao, H.; Wang, H.; Chen, L.; Li, Y.; Sotelo, M. A. Li, Z. (2021). YOLOv4-5D: An effective and efficient object detector for autonomous driving, *IEEE Transactions on Instrumentation and Measurement*, 70, 1–13, 2021.
- [3] Ding, Y.; Li, W.; Zhu, Y. (2021). Lane Line Detection Based On YOLOv4, *In2021 IEEE International Conference on Signal Processing, Communications and Computing (ICSPCC)*, 1–5, 2021.
- [4] Fan, Y. C.; Yelamandala, C. M.; Chen, T. W.; Huang, C. J. (2021). Real-Time Object Detection for LiDAR Based on LS-R-YOLOv4 Neural Network, *Journal of Sensors*, 2021, 2021.
- [5] Guo, J.; Liu, C.; Cao, J.; Jiang, D. (2021). Damage identification of wind turbine blades with deep convolutional neural networks, *Renewable Energy*, 174, 122–133, 2021.
- [6] Haris, M.; Hou, J.; Wang, X. (2021). Multi-scale spatial convolution algorithm for lane line detection and lane offset estimation in complex road conditions, *Signal Processing: Image Communication*, 99, 116413, 2021.
- [7] He, K.; Zhang, X.; Ren, S.; Sun, J. (2020). Deep residual learning for image recognition, *Proceedings of the IEEE conference on computer vision and pattern recognition*, 770–778, 2016.
- [8] Haris, M.; Hou, J.; Wang, X. (2022). Lane Lines Detection under Complex Environment by Fusion of Detection and Prediction Models, *Transportation Research Record*, 2676(3), 342–359. 2022.
- [9] Kuang, X.; Sui, X.; Liu, Y.; Chen, Q.; Gu, G. (2022). Single infrared image enhancement using a deep convolutional neural network, *Neurocomputing*, 332, 119–128, 2019.
- [10] Ko, Y.; Lee, Y.; Azam, S.; Munir, F.; Jeon, M.; Pedrycz, W. (2021). Key points estimation and point instance segmentation approach for lane detection, *IEEE Transactions on Intelligent Transportation Systems*, 23(7), 8949–8958, 2021.
- [11] Kavya, R.; Hussain, K. M. Z.; Nayana, N.; Savanur, S. S.; Arpitha, M.; Srikantaswamy, R. (2021). Lane Detection and Traffic Sign Recognition from Continuous Driving Scenes using Deep Neural Networks, *2021 2nd International Conference on Smart Electronics and Communication (ICOSEC)*, 1461-1467, 2021.
- [12] Li, W.; Qu, F.; Liu, J.; Sun, F.; Wang, Y. (2020). A lane detection network based on IBN and attention, *Multimedia Tools and Applications*, 79(23), 16473–16486, 2020.
- [13] Luo, S.; Zhang, X.; Hu, J.; Xu, J. (2020). Multiple lane detection via combining complementary structural constraints, *IEEE Transactions on Intelligent Transportation Systems*, 22(12), 7597–7606, 2020.

- [14] Li, X.; Yun, X.; Zhao, Z.; Zhang, K. ; Wang, X. (2022). Lightweight Deeplearning Method for Multi-vehicle Object Recognition. *Information Technology and Control, Sensors*, 51(2), 294–312, 2022.
- [15] Lu, K.; Li, J.; Zhou, L.; Hu, X.; An, X.; He, H. (2018). Generalized haar filter-based object detection for car sharing services, *IEEE Transactions on Automation Science and Engineering, IEEE Transactions on Geoscience and Remote Sensing*, 15(4), 1448–1458, 2018.
- [16] Muthalagu, R.; Bolimera, A., Kalaichelvi, V. (2020). Lane detection technique based on perspective transformation and histogram analysis for self-driving cars, *Computers & Electrical Engineering*, 85, 106653, 2020.
- [17] Neil, J.; Cosart, L.; Zampetti, G. (2021). Precise timing for vehicle navigation in the smart city: an overview, *IEEE Communications Magazine*, 58(4), 54–59, 2021.
- [18] Qi, Y.; Yang, Z.; Sun, W.; Lou, M.; Lian, J.; Zhao, W.; Deng, X.; Ma, Y.; Y. Ma. (2022). A comprehensive overview of image enhancement techniques, *Archives of Computational Methods in Engineering*, 29, 583–607, 2019.
- [19] Ryu, S. E.; Chung, K. Y. (2022). Detection Model of Occluded Object Based on YOLO Using Hard-Example Mining and Augmentation Policy Optimization, *Applied Sciences*, 11(15), 7093, 2022.
- [20] Song, W.; Yang, Y.; Fu, M.; Li, Y.; Wang, M. (2018). Lane detection and classification for forward collision warning system based on stereo vision, *IEEE Sensors Journal*, 18(12), 5151–5163, 2018.
- [21] Tang, J.; Li, S.; Liu, P. (2021). A review of lane detection methods based on deep learning, *Pattern Recognition, Pattern Recognition, Pattern Recognition*, 111, 107623, 2021.
- [22] Viola, P.; Jones, M. (2001). Rapid object detection using a boosted cascade of simple features, *In Proceedings of the 2001 IEEE computer society conference on computer vision and pattern recognition*, 2001.
- [23] Wu, J., Xu, H., Zhao, J. (2018). Automatic Lane identification using the roadside LiDAR sensors, *IEEE Intelligent Transportation Systems Magazine*, 12(1), 25–34, 2018.
- [24] Wang, H.; Wang, Y., Zhao, X.; Wang, G., Huang, H.; Zhang, J. (2019). Lane detection of curving road for structural highway with straight-curve model on vision, *IEEE Transactions on Vehicular Technology*, 68(6), 5321–5330, 2019.
- [25] Yoo, J.; Kim, D. (2021). Graph model-based lane-marking feature extraction for lane detection, *Sensors, IEEE Transactions on Vehicular Technology*, 21(13), 4428, 2021.
- [26] Ye, X. Y.; Hong, D. S.; Chen, H. H.; Hsiao, P. Y.; Fu, L. C. (2022). A two-stage real-time YOLOv2-based road marking detector with lightweight spatial transformation-invariant classification, *Image and Vision Computing*, 102, 103978, 2020.
- [27] Yang, W.; Zhang, X.; Lei, Q.; Shen, D.; Xiao, P.; Huang, Y. (2020). Lane Position Detection Based on Long Short-Term Memory (LSTM), *Sensors*, 20(11), 3115, 2022.
- [28] Zhou, T.; Yang, M.; Jiang, K.; Wong, H.; Yang, D. (2020). MMW radar-based technologies in autonomous driving: A review, *Sensors*, 20(24), 7283, 2020.
- [29] Zhao, Z.; Wang, Q.; Li, X. (2020). Deep reinforcement learning based lane detection and localization, *Neurocomputing*, 413, 328–338.
- [30] Zou, Q.; Jiang, H.; Dai, Q.; Yue, Y.; Chen, L.; Wang, Q. (2019). Robust lane detection from continuous driving scenes using deep neural networks, *IEEE transactions on vehicular technology, Signal Processing: Image Communication*, 69(1), 41–54, 2019.

- [31] Zhang, X.; Yang, W.; Tang, X.; Liu, J. (2018). A fast learning method for accurate and robust lane detection using two-stage feature extraction with YOLOv3, *Sensors*, 18(12), 4308, 2018.
- [32] Zhang, Z. D.; Tan, M. L.; Lan, Z. C.; Liu, H. C.; Pei, L.; Yu, W. X. (2022). CDNet: a real-time and robust crosswalk detection network on Jetson nano based on YOLOv5, *Neural Computing and Applications*, 34, 10719—10730, 2021.



Copyright ©2022 by the authors. Licensee Agora University, Oradea, Romania.

This is an open access article distributed under the terms and conditions of the Creative Commons Attribution-NonCommercial 4.0 International License.

Journal's webpage: <http://univagora.ro/jour/index.php/ijccc/>



This journal is a member of, and subscribes to the principles of,
the Committee on Publication Ethics (COPE).

<https://publicationethics.org/members/international-journal-computers-communications-and-control>

Cite this paper as:

Gao, S.; Wang, S.; Pan, W.; Wang, M.; Gao, S. (2022). Based on Haar-like feature and improved YOLOv4 navigation line detection algorithm in complex environment, *International Journal of Computers Communications & Control*, 17(6), 4910, 2022.

<https://doi.org/10.15837/ijccc.2022.6.4910>